Lipid Nanotubes: A Unique Template To Create Diverse One-Dimensional Nanostructures†

Yong Zhou‡ and Toshimi Shimizu*,‡,§

SORST, Japan Science and Technology Agency (JST), Tsukuba Central 5, 1-1-1 Higashi, Tsukuba, Ibaraki 305-8562, Japan, and Nanoarchitectonics Research Center (NARC), National Institute of Advanced Industrial Science and Technology (AIST), Tsukuba Central 5, 1-1-1 Higashi, Tsukuba, Ibaraki 305-8565, Japan

Received July 25, 2007. Revised Manuscript Received October 12, 2007

Lipid molecules can self-assemble in liquid media into open-ended, hollow cylindrical structures, which are composed of rolled-up bilayer membrane walls. The resultant lipid nanotubes (LNTs) have a few unique properties, such as controllable diameters and length and finely functionalizable surfaces benefitting template-synthesized one-dimensional (1-D) nanostructures, that no other individual templates possess. The elegant hollow cylinders of the LNT can modulate the nucleation, growth, and deposition of inorganic substances on their external and internal surfaces, in the hollow cylinder, and in the bilayer membrane wall. Templating the LNTs enables one to produce diverse 1-D nanostructures, such as nanotubes, concentric tubular hybrids, complex helical architectures, and 1-D arrays of quantum dots.

1. Introduction

The fabrication of one-dimensional (1-D) nanostructures is currently one of the most attractive subjects in nanomaterial fields.[1–3] In particular, the applicative needs for high-aspect-ratio nanomaterials motivate the excellent fabrication of mesoscopic nanodevices, such as nanotubes, nanowires, nanorods, nanoribbons, and 1-D nanodot arrays. Such 1-D nanostructures provide a good system to investigate electrical, thermal, or mechanical properties that are produced as a direct consequence of their size, shape, and reduced dimensionality. An impressive variety of methodologies have been developed to make the 1-D nanostructures, most of which may be classified into so-called soft- and hard-template syntheses.[4,5] The soft-template method generates the 1-D nanostructures usually in solutions that contain functional surfactants or polymers directing the growth of certain crystal faces of the materials. The hard-template method represents a straightforward route resulting in 1-D nanostructures. In this approach, the templates simply serve as scaffolds, where different 1-D materials form by replication or nanocasting. The advantage of the hard-template method is its ability to produce complex 1-D nanostructures and facile control of the composition and dimension. As the 1-D hard templates, channels within porous membranes,[6] supramolecular structures that self-assembled from organic amphiphiles or block copolymers,[7] biomolecules like DNA,[11] protein microtubules,[12] and the tobacco mosaic virus[10] have been widely used so far. Lipid nanotubes (LNTs) are also becoming promising templates that provide discrete, organic, tubular assemblies made of an extremely large number of identical lipid molecules.[11]

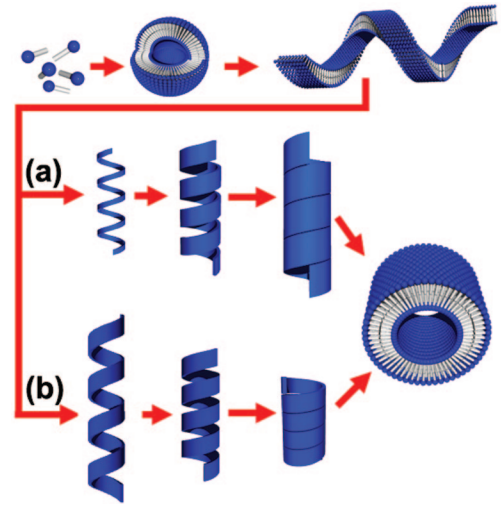

Figure 1. Formation mechanism of a LNT based on chiral molecular self-assembly.

Lipid is the basic building block of biological membranes. In liquid media, lipid molecules self-assemble into diverse aggregate morphologies, depending on the molecular shape and solution condition such as the lipid concentration, electrolyte concentration, pH, and temperature.[12] A limited number of lipid molecules can self-assemble into open-ended, hollow cylindrical structures, which are composed of rolled-up bilayer membranes.[13] This potential architecture can be considered one of the largest self-organized nonliving structures yet observed. The LNT formation occurs commonly in two steps, as represented in Figure 1: (i) the formation of intermediate bilayer ribbons in solutions through the morphological change of vesicles in a cooling process and (ii) coiling of the solid bilayer ribbon into an open helix, which eventually closes to yield nanotubes by either widening of the tape width and maintenance of a constant helical

† Part of the "Templated Materials Special Issue".

* To whom correspondence should be addressed. Fax: +81-29-861-4545. E-mail: tshmz-shimizu@aist.go.jp.

‡ JST.

§ AIST.

10.1021/cm701999m CCC: $40.75
Published on Web 12/06/2007

pitch (Figure 1a) or shortening of the helical pitch of the ribbon and maintenance of a constant tape width (Figure 1b).[11] The driving force for the solid bilayer formation and the subsequent coiling into the nanotube are chiral interactions of constituent molecules, which force them to pack at a nonzero angle with respect to their nearest neighbors in the bilayer membranes. This situation leads to spontaneous torsion and resultant coiling of the edges of the bilayer membrane and eventually the formation of a cylindrical hollow. Different from the common formation scheme of the LNTs mentioned above, wedge-shaped bolaamphiphilic molecules have a tendency to directly assemble into hollow cylindrical structures without forming helically twisted or coiled ribbons during the course of self-assembly.[14]

The LNTs have a few unique properties benefitting template-synthesized 1-D nanostructures that no other individual templates possess: (1) Such tubular structures are of interesting hydrophilic internal and external membrane surfaces, in sharp contrast to carbon nanotubes. Furthermore, one can provide asymmetrical inner and outer surfaces as well as identical ones. Those advantages make them ideal candidates for controlled release, chemical reaction, selective filling of nanomaterials, and so on. (2) The diameters of the LNTs characteristically span the region between 10 and 1000 nm, and most of the inner diameters fall in the 10–200 nm range. Neither top-down-type microfabrication procedures nor any fabrication methods for both carbon nanotubes (1–10 nm)[15] and molecular hollow cylinders such as cyclodextrin[16] and cyclic peptide nanotubes (<1 nm)[17] can generate tubular structures with these dimensions. The ability to precisely control the inner and outer diameters, length, and wall thickness in a wide range from several nanometers to micrometers allows one to directly determine their suitability for diverse technological applications.[14,18–23] Spector et al. claimed that reducing the LNT membrane thickness may cut the lipid material cost by at least 80% in practical applications.[24] (3) Incorporation of desired functional groups into lipid monomers allows the outer and inner surfaces of the LNT to be functionalized and modified.[14b,c] (4) The LNTs can be easily manipulated, positioned, and aligned on diverse substrates with various techniques including microextrusion,[25] microfluidic network,[26,27] magnetic field,[28,29] and biorecognition.[30]

The LNTs can modulate the nucleation, growth, and deposition of extensive sorts of inorganic substances. Templating the different parts (outer and inner surfaces, hollow cylinders, and bilayer membrane walls) of the self-assembled LNT architectures can produce a proliferation of 1-D structures with potential applications, as summarized in Figure 2 and Table 1. Uniform growth of size- and shape-controlled nanodots (NDs) on the surfaces of the LNTs gives rise to nanotubes with tunable functions (Figure 2, part 1). Sol–gel reaction of inorganic substances on the outer and inner surfaces may create both inorganic nanotubes and concentric tubular hybrids (Figure 2, part 2). Crystallization and deposition of functional NDs in the bilayer membrane wall allows for the generation of a specific tubular nanocomposite (Figure 2, part 3). Utilization of the chiral packing of lipid molecules in the LNTs allows for the formation of complexed helical organization of species (Figure 2, part 4). Encapsulation of nanoobjects in the hollow cylinder of the LNTs may produce their 1-D arrays (Figure 2, part 5). This short review represents recent progress in the creation of diversities of the LNT-templated 1-D nanostructures.

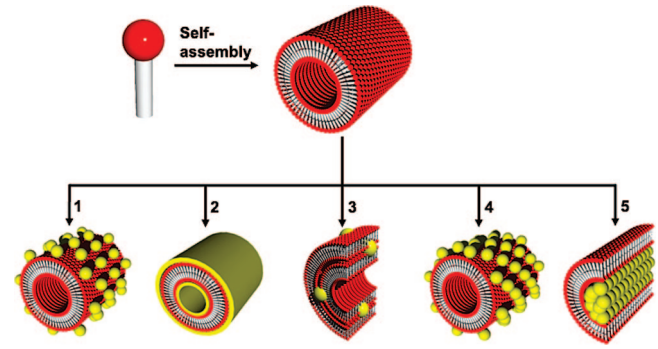

Figure 2. Schematic illustration for the various templating features of LNTs: (1) surface modification; (2) organic–inorganic hybrids; (3) crystallization and/or deposition in bilayer membrane walls; (4) helical organization; (5) confinement. The objects displayed in yellow indicate templated structures.

2. Functional Nanotubes by Templating of LNT Surfaces

The early report that addressed the templating applications of LNTs was carried out in Schnur's research group. The LNT derived from 1,2-bis(tricosa-10,12-diynoyl)-*sn*-glycero-3-phosphatidylcholine, **1**(*8,9*), acted as an excellent scaffold to create metal nanotubes by coating the LNT with an elegant electroless plating process. The electroless metallization technique allows the nanotubes to be clad on the exterior and interior surfaces with a uniform layer of metals. Nonconductive surfaces undergo activation with Pd^{2+} and Sn^{2+}, followed by immersion in a deposition bath that comprises metal ions and reductant.[31] Changes in the concentration of the plating solution and in the plating time allow for control of the thickness of the metal layer, typically ranging from 20 to 200 nm. The LNT can be metallized with any metals capable of being plated. By plating on the LNT an electrically conducting metal such as Cu^{2+},[32] highly electrically conducting nanotubes can be formed. Similarly, by plating a magnetic metal such as Ni^{2+}, one can obtain the nanotubes of low electrical conductivity but of high magnetism. Plating of both an electrically conducting metal and a magnetic metal with an overplating process, i.e., deposition of another metal on the initial metal coat, allows the LNT to possess high electrical conductivity and high magnetism.[33] The hollow metal microcylinders thus produced have potential applications in microwave[34] and long-term sustained-release systems in agriculture, environment, and medicine.[35]

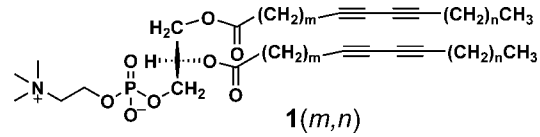

Besides the electroless plating technique, Matsui et al. utilized hydrogen bonding as an interactional force to uniformly coat the peptidic LNT of bis(*N*-α-amidoglycylglycine)-1,7-heptanedicarboxylate **2**(*7*) with gold nanocrys-

Table 1. LNT Templating and the Location for Diverse 1-D Nanostructures with Potential Applications

chemical phenomena	location of occurrence	templated materials	applications
1. surface modification	outer and inner surfaces	Cu,[31–33,39a] Ni,[31–33,39b] Au,[36,41,43] Ag,[40] ZnS[42]	controlled release, sensor, nanocircuit, etc.
2. sol–gel reaction	outer and inner surfaces	aluminum carbonate,[44] silica,[45,48–50,53,58] Fe_3O_4,[46] silicate clay,[47] TiO_2,[51,52b] Ta_2O_5,[51] V_2O_5[51]	photocatalysis, reinforcement of materials, etc.
3. crystallization and deposition	bilayer membrane walls	CdS,[54] Pt[57]	fluorescence tracer in biological systems, catalysis, etc.
4. helical organization	outer and inner surfaces	Au,[70] silica,[71] Cu,[73] Pd,[74] CdS,[75] Ppy,[76,77] PEDOT,[77] poly(aniline),[77] streptavidin,[78,79] ferritin[79]	catalysts, helical sensors, optical materials, springs and inductors for microelectronic devices, etc.
5. confinement	hollow cylinder	Fe_3O_4,[84,85,91] Au,[54,88,93] Ag[88,92] CdS,[89] ferritin,[14b,c,54,90] polymer beads,[14b] DNA,[14c]	nanochannel, metal nanowire, storage nanovessel, nanoreactor, capacitor, fundamental study of electrical transport and optical phenomena, etc.

tals.[36] That LNT was initially synthesized by our own research group,[37] proving to give vesicle-encapsulated microtubes. The gold nanocrystal capped with 11-mercaptoundecanoic acid [$HS(CH_2)_{10}COOH$] was mixed in an ethanol solution with the LNT of **2**(*7*). After the resulting solution was aged overnight, they found that hydrogen bonding between the amide groups of the LNT and the carboxylic acid groups on the gold nanoparticle drives the nanocrystal to deposit on the LNT surface. The same group also grew a series of uniform and isotropic metal nanocrystals on the LNT of **2**(*7*) by immobilizing a "mineralizing peptide" on the nanotubes.[38] Those immobilized peptides with particular sequences, having biological recognition toward specific metal ions, are able to dominate nanoparticle nucleation and phase stabilization. By varying the peptide conformations and charge distributions sensitive to the pH and ion concentrations of the growth solution, they succeeded in controlling the size,[39] shape,[40] packing density, particle-to-particle distance,[41] and phase structure of the coating nanocrystals.[42] Coating the peptidic LNT, which possesses a selected diameter comparable to the size of metal nanoparticles, gives a 1-D single-chain model of the nanoparticle.[43]

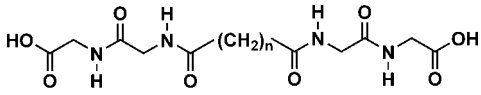

2(*n*)

The tubular architectures of lipids can serve as templates for mineral nucleation and deposition of inorganic nanostructures. The deposition or coating of such inorganic substances occurs concurrently at both the inner and outer surfaces. Aluminum carbonate[44] and silica[45] that grow on the nanotube of **1**(*8*,*9*) result in continuous coating over the entire nanotube surface. Mann and co-workers fabricated magnetic and nonmagnetic iron oxides with a sugar-based lipid galactocerebroside **3**, doped with small amounts of an anionic sulfated derivative **4**.[46] The incorporation of sulfate into the neutral tubelike assemblies provides the microstructure with anionic sites for electrostatic binding of Fe^{3+} polyhydroxy cationic species, inducing the subsequent nucleation of the iron oxides onto the LNT surface. Mann's group also reported a nanometer-thick, continuous coating of a magnesium phyllo(organo)silicate clay containing a covalently linked ethylenediaminopropyl moiety using self-assembled nanotubes of **1**(*8*,*9*) as templates.[47] This report was the first to address control of the deposition of organically functionalized layer materials. Our own research group explored a direct sol–gel replication based on the self-assembled peptidic LNT of **5** with a single bilayer wall in aqueous solutions.[48] Conventional sol–gel reaction requires active solution catalysts such as H^+ or OH^-. However, the weakly acidic and mildly catalytic lipid headgroup, with the aid of a minimal amount of positive charges on the LNT surface, cause the deprotonated silica precursor and tetraethyl orthosilicate (TEOS) to be adsorbed on the LNT surface by electrostatic force. The reaction mixture underwent subsequent hydrolysis and condensation in the absence of any additional catalysts. After the adsorption process has reached its isoelectric point, the template may lose its function as a catalyst and the sol–gel reaction would almost end. The silica nanotubes produced in this way have ultrathin walls of approximately 8–15 nm, which contrast with thicker 30 nm walls promoted in the presence of a small amount of OH^- as a base catalyst. A change in the ratio of the LNT to TEOS allows us to control the wall thickness of the silica nanotubes within as little as 4 nm precision.[49] It was found that the diameter of the LNT of **5** decreases with the addition of ethanol, which affects the nature of hydration layers surrounding the bilayer of **5** and alters the spacing and packing of the lipid headgroup.[50] We utilized such solvent-sensitive diameters to regulate the silica nanotube diameters in the 30−80 nm range, which depend on the amount of ethanol. Sol–gel reaction using the peptidic nanotube of **5** as a template was also feasible to synthesize transition-metal-oxide nanotubes including titanium oxide, tantalum oxide, and vanadium oxide.[51] The reaction rate of the precursor of the transition-metal oxide in hydrolysis and condensation is about 5 orders of magnitude faster than that of the silica precursor. Therefore, the aqueous LNT solution was frozen in liquid nitrogen for a few seconds to slow the hydrolysis rate of the metal precursors. The iced LNT possesses an unfrozen water layer around the LNT surface. When the iced LNT begins to melt, the ethanol solution of the precursors would permeate into this unfrozen water layer. The positive charge of the LNT promotes the adsorption of the inorganic precursor onto the surface of the LNT. The precursor also promotes the sol–gel reaction and leads to metal nanotubes with smooth surfaces. However, the use of an iced neutral LNT that self-assembled from *N*-(11-*cis*-octadecenoyl)-β-D-glucopyranosylamine (**6**) only produced metal nanorods consisting of the metal nanoparticle aggregates.[52] This finding means that the sol–gel reaction is confined to the

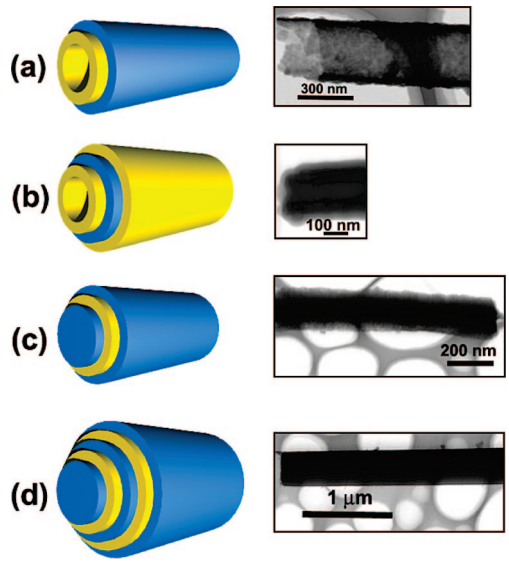

Figure 3. Schematic illustration (left) and the corresponding STEM images (right) for the concentric tubular hybrids consisting of cylindrical layers of (a) silica (shown in blue)−lipid (shown in yellow), (b) lipid−silica−lipid, (c) silica−lipid−silica, and (d) silica−lipid−silica−lipid−silica, where the lipid **6** self-assembles on silica nanotube templates. The STEM images were reproduced with permission from ref 53. Copyright 2005 Royal Society of Chemistry.

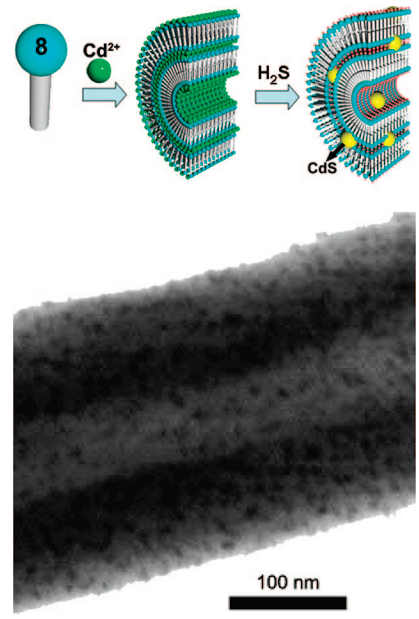

Figure 4. Schematic illustration (top) and STEM image (bottom) for the LNTs of **8**, where the CdS NDs are embedded all over the lipid bilayer membranes. The STEM image was reproduced with permission from ref 54. Copyright 2007 Wiley-VCH.

unfrozen water layer surrounding the LNT but does not occur on the surface of the LNT because of the neutral surface charge of the LNT of **6**.

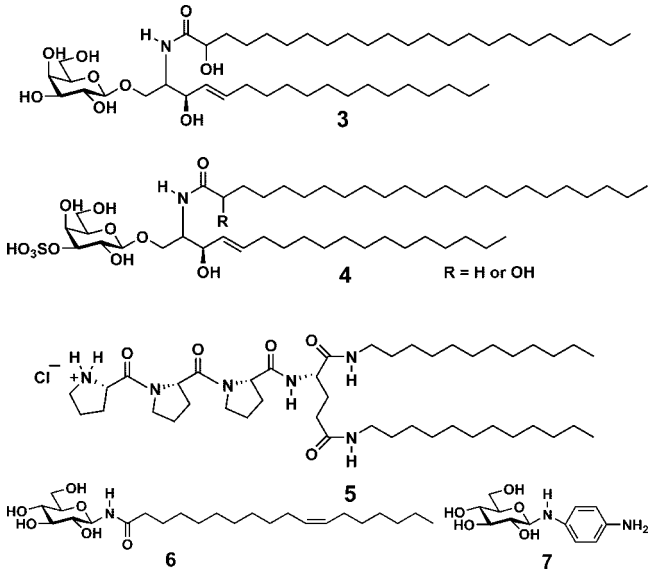

3. Organic–Inorganic Tubular and Ribbon Hybrids

Organic–inorganic hybrids can show not only combined properties of original components but also improved performances not seen in original components. Therefore, such nanocomposites act as important materials to build electrical and optical nanodevices. While considerable work has accomplished three-dimensional (3-D) bulky and two-dimensional (2-D) hybrids, the fabrication of 1-D hybrid materials is still difficult because of challenging techniques. We yielded a variety of concentric tubular hybrids, consisting of cylindrical layers of silica−lipid (Figure 3a), lipid−silica−lipid (Figure 3b), silica−lipid−silica (Figure 3c), and silica−lipid−silica−lipid−silica (Figure 3d), using self-assembly of **6** on silica nanotube templates.[53] Self-assembly of **6** in the interior nanospace of hollow cylindrical silica nanotubes produced a hybrid nanotube consisting of two concentric layers: one is silica and the another lipids. Doping of (aminophenyl)-β-D-glucopyranoside (**7**) into the lipid **6** induced concomitant self-assembly of lipid layers on both the inner and outer surfaces of the silica nanotube, producing hybrid nanotubes with concentric lipid−silica−lipid walls. Subsequent sol–gel reaction using these lipid−silica−LNTs as templates resulted in the formation of more complexed hybrid nanotubes with a concentric five-layered structure of silica−lipid−silica−lipid−silica. One can expect that these kinds of hybrid tubular structures and hybridization methods will be useful in a wide variety of applications.

Besides the surface and hollow cylinder of the LNT, the bilayer membrane wall also serves as an embedding matrix of NDs to form functional nanotubes. We have made fluorescent nanotubes from a synthetic peptide lipid, the sodium salt of 2-[2-(2-tetradecanamidoacetamido)acetamido]acetic acid (**8**),[54] which consists of CdS-embedded bilayer membranes. The lipid **8** can self-assemble in aqueous solutions into a hollow cylindrical structure in the presence of proton (H^+) (H-LNT) or a series of transition-metal cations (M-LNT).[55] As illustrated in Figure 4, coordination of Cd^{2+} to two negatively charged COO^- groups of the lipid **8** allows it to form a Cd-complexed LNT (Cd-LNT). Upon exposure to H_2S vapor, the Cd^{2+} in the Cd-LNT was released as a result of competitive binding of the proton to the COO^- group, resulting in the formation of H-LNT. The released Cd^{2+} subsequently reacted with S^{2-} to initiate CdS nuclei and finally grew into the CdS NDs all over the lipid bilayer membranes. The scanning transmission electron microscopy (STEM) image reveals that the CdS NDs have an average diameter of around 4−5 nm with narrow distribution and

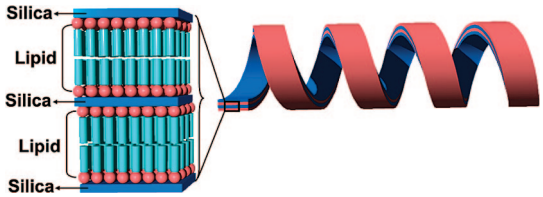

Figure 5. Schematic illustration of a helical silica−lipid ribbon nanocomposite with a coiled multilamellar architecture.

separate from one another without any aggregation. The tubular nanocomposites clearly exhibited distinguishable fluorescence originating from electronic transition of the CdS NDs. The fluorescence is resistant to photobleaching compared to other organic moiety-based fluorescence and enables one to visualize for a long time and to trace the localization in biological systems. The fluorescent CdS-LNT has proved to successfully act as a supramolecular nanotube host to encapsulate ferritin and gold nanoparticles, which are applicable for the delivery of biomolecules. Removal of the organic moiety of the M-LNT by calcination in air allows us to obtain diverse metal oxide nanotubes.[55] Song et al. produced a peptide nanotube of porous walls, which self-assembled from the NH_2−Phe−Phe−COOH peptide molecules,[56] by simplifying Reches and Gazit's method.[57] The pores allow an aqueous K_2PtCl_4 solution to freely diffuse into all regions within the bilayer membrane walls. The addition of ascorbic acid results in the reduction of the metal ion and subsequently the formation of small platinum nanoparticles embedded in the nanotube walls. The Pt−peptide nanocomposite has many potential applications, e.g., catalysis, electronics, and optics.

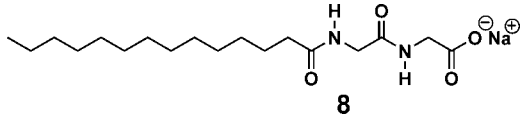

8

A synergistic co-assembly process of **1**(*8,9*) with TEOS in ethanol forms a silica−lipid helical ribbon biphase, in which the lipid bilayers were intercalated with thin sheets of amorphous silica (Figure 5).[58] Unlike conventional template processes using the sol–gel reaction, hydrolysis and condensation of TEOS by the acid catalyst were specifically associated and coupled with the self-assembly of the lipid molecules. This finding indicates that templating of the silica helical nanostructure takes place even between lipid bilayers and the co-assembly leads to stabilization of the metastable ribbon.

4. Complex Helical Architectures by Tracing LNTs

One of the most impressive features with LNTs as templates for the formation of inorganic nanostructures is to produce helical architectures. Naturally occurring helices are the most fascinating objects of interest in biology. They are sometimes involved with chiral molecular configuration (primary structure) and sometimes are featured by helical chain conformation (secondary structure), helical molecular assemblies (tertiary structure), and the chiral phase (quaternary structure).[59] Striking DNA and RNA in nature self-assemble into single-, double-, and triple-helical structures. The functional inorganic materials of helical structures have

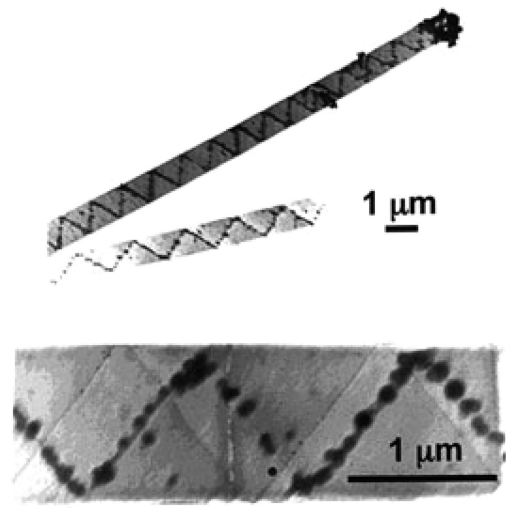

Figure 6. TEM images of nanoparticle helices inside the nanotubes of **1**(*8,9*) (98%) and **9** (2%) after the PEI^+/PSS/PEI^+/(45 nm SiO_2) treatment. The tube diameter was 1 μm. Reproduced with permission from ref 71. Copyright 2000 American Chemical Society.

wide utilization as asymmetric reaction catalysts,[60] helical sensors,[61,62] optical materials,[63,64] and so forth. However, the 1-D inorganic structure with a helical sense is difficult to fabricate artificially. Templating LNTs along with some chiral organogel systems[65–68] is an effective route to creating diverse inorganic helical structures. LNTs often exhibit helical markings that wind around the cylinders,[69] reminiscent of chiral self-assembly involving a helically coiled ribbon structure as an intermediate. The lipid molecules residing at the edge sites along the helical marking exhibit a stronger chemical activity than those sited within the lamellar bilayer sheets, probably because of the high surface energy associated with the curved edges. This character makes the helical seams much better candidates for adsorption of exterior objects than the other surface of the nanotube and allows the adsorbed objects to trace the chemically patterned organic surface for helical organization. Burkett and Mann observed a clear helical pattern of gold nanoparticles on the LNT of **1**(*8,9*).[70] They reduced $HAuCl_4$ in the presence of the LNT. The obtained gold nanoparticles traced the underlying helical ribbon edge of the nanotube and organized along the longitudinal seam of the LNT. Beautiful helices of SiO_2 nanoparticles were made in the interior of the nanotubes of **1**(*8,11*), mixed with 2% of the charged lipid **9**(*8,9*) (Figure 6).[71] By the multistage layer-by-layer (LBL) adsorption process of PEI^+/PSS^-/PEI^+ [PEI = poly(ethylenimine) and PSS = poly(styrenesulfonate)] to induce positive charge on the nanotubes,[72] the negatively charged SiO_2 nanoparticles of 45 nm are absorbed along a charged line defect of the interior surface of the nanotubes. This finding revealed that the charged lipids concentrate along helical defect lines that are not otherwise visible and provide anchoring points for the assembly of PEI^+/PSS^-/PEI^+/SiO_2^-. A metallic copper spiral/helical nanostructure was prepared with the same LBL route combined with selectively electroless metallization.[73] Negatively charged nanoparticles of a palladium catalyst bonded to the terminal cationic layer of the PEI multilayer film and then initiated selective template metallization of copper on nanoscale seams of the

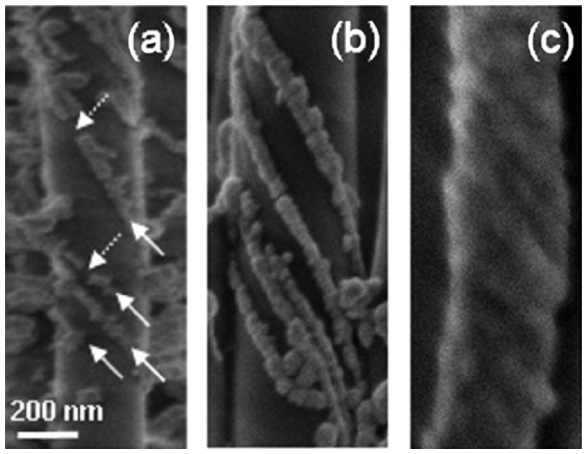

Figure 7. Time-resolved high-resolution field emission saccnning electron microscopy images that show the formation of the helical array of CdS nanoparticles on the LNT surface of **6** for (a) 3 h, (b) 5 h, and (c) 1 day. Reproduced with permission from ref 75. Copyright 2006 American Chemical Society.

LNT to form the helical nanostructure. The metal spiral structures are potentially useful as springs or inductors for microelectromechanical system devices and interlocking reinforcements for composite materials. A helical array of palladium nanoparticles was formed in the presence of the helical ribbon, which self-assembled from a cholesterol derivative doped with a diaminoethylene glycol moiety **10**.[74] Adsorption of Pd^{II} ions onto the edge sites of the helical ribbon, followed by subsequent reduction with ascorbic acid, gives rise to palladium nanoparticles tracing the helical edge of the ribbon.

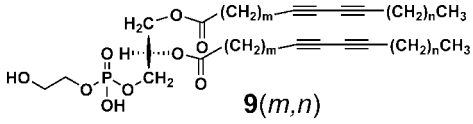

9(*m*,*n*)

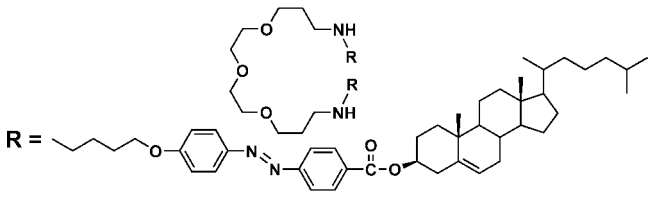

10

Besides the helical patterns of metal, arrayed CdS NDs, which locate helically on a chiral template of glycolipid nanotubes consisting of the binary components **6** and **7**, were made by our own research group.[75] The LNT of **6** was functionalized by incorporation of **7** as an additive through the binary self-assembly. This functionalization process created active binding sites, which trace the chiral molecular packing of the nanotube. At the initial stage, CdS selectively nucleated and grew into nanoparticles on the LNT (Figure 7a). These nanoparticles connected one by one in a 1-D pattern, twining the curved surface of the LNT scaffold, as marked by solid arrows. The existence of a gap between the sections (shown as dotted arrows) indicates that there are many nucleation sites in the 1-D growth track along the LNT. With reaction time, the discontinuous connection of the nanoparticles evolved into chainlike and nanowire-like

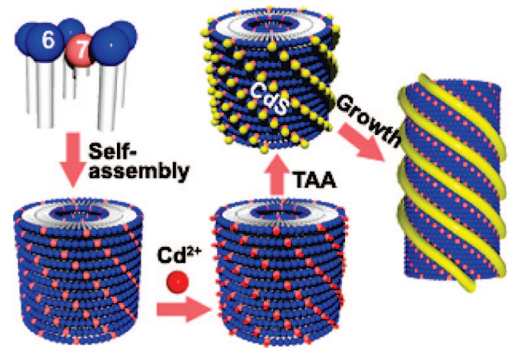

Figure 8. Illustration of the formation mechanism for the helical arrays of CdS nanoparticles on the LNT surface of **6**.

architectures along the scaffold (Figure 7b). After 1 day of incubation, the helical array of the CdS nanoparticles on the LNT formed (Figure 7c). On the basis of the theoretical model for chiral self-assembly of LNTs,[11] we can deduce that the nanotube structure from **6** has the molecular tilt optimally oriented at an angle of 45°. Thus, it is expected that **7** is also distributed in a helical fashion within the LNT membrane, as shown in Figure 8. As a result, Cd^{2+} will helically nucleate on the surface of the functionalized LNT through preferential affinity of Cd^{2+} to the amino group of **7**. Interaction with S^{2-}, slowly released by decomposition of thioacetamide (TAA), allows the heterogeneous nucleation of CdS along the surface of the LNT. An increase in the incubation time promoted the growth of the nuclei into nanoparticles and eventually the formation of chain- or wirelike architecture helically twinning the LNT. The left-handed helical sense of the CdS chains on the LNT suggests the identical helical sense of the chiral molecular packing.

Because organic monomers often produce cationic intermediates in their oxidative polymerization processes, the edges/seams of the anionic LNTs can also direct the polymerization of the monomers into helical polymers by electrostatic attractive force. Pyrrole (py) was conducted to chemically polymerize in the presence of the LNT of **1**(*8*,*9*).[76] The polymerization process exclusively occurred on the edges (or seams) of the LNT. The cationic nuclei of poly(pyrrole) (Ppy) initially formed in the solution and then precipitated out from the solution. Ppy subsequently deposited onto the lipid edges selectively, where the exposed electron-rich acyl and acetylene groups may offer chemically preferred sites for adsorption. Eventually, the polymerization proceeds preferentially along the edges. The growing Ppy strands exhibited long helical forms made up of coalesced beads. Shinkai et al. created more elegant helical tapes and intertwined helical structures of diverse conjugate polymers including poly(ethylenedioxythiophene) (PEDOT), Ppy, and poly(aniline) using lipid fibrous assemblies with helical motifs as templates.[77] The cationic intermediates, which were produced by electro-oxidative or chemical-oxidative polymerization of these monomers, adsorbed onto the anionic lipid assemblies **11** and **12** to trace the helical structures. Both the right- and left-handed helical structures were produced by a change in the hydrophilic headgroup of the lipid.

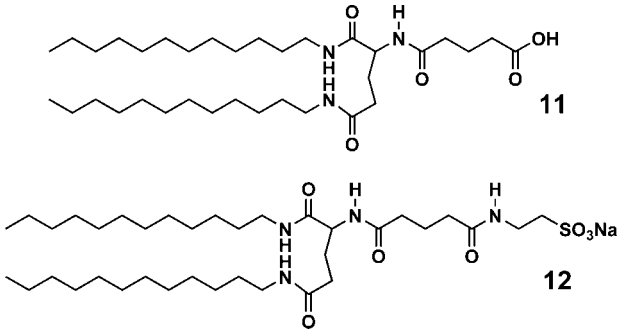

The constituent molecules of LNTs generally have binding affinity to biomolecules such as proteins. This renders LNTs the ability to helically crystallize a wide variety of proteins. Streptavidin bonded to a biotinylated LNT and spontaneously assembled into ordered helical arrays at the nanotube surface.[78] These crystals exhibit regular order up to about 1.5 nm resolution. The tubular crystal is distinct in nature from other tubular crystals of proteins and allows its 3-D structure to be calculated from one single image by Fourier−Bessel reconstruction methods.[79] In addition, the helical crystals of proteins can be transferred onto the grids for electron microscopy more easily than 2-D crystals of proteins can. The helical arrays of streptavidin further act as functionalized supramolecular devices that bind a number of biotinylated objects such as ferritin.[80]

5. 1-D ND Arrays Confined to LNT Hollow Cylinders

Nanoparticle synthesis in engineered organic micro- and submicroreactors, such as vesicles, micelles, and polyelectrolyte capsules, has attracted gradually increasing attention.[81] LNT can provide a 1-D hollow cylindrical environment with a high axial ratio, favoring the encapsulation and 1-D confinement of appropriate nanostructures with dimensions in the single-nanometer range.[82,83] There are two general paths to realize the 1-D arrangement of the NDs in the LNT, as illustrated in Figure 9. In path I, when a lyophilized LNT is dispersed into the aqueous solution containing liquid-soluble NDs, the fluidic NDs may diffuse into the hollow cylinder of the LNT driven via electrostatic absorption, capillary force, and other interactions between LNT hosts and loaded guests. Letelliner et al. observed the distribution of charged magnetic nanoparticles around the nanotubes of **1**(*8*,*9*).[84] They used a single stage of treatment with magnetic nanoparticles of maghemite iron oxide with a diameter of 7 nm. These particles carried either a positive or a negative charge, depending on the pH. They found that the positively charged particles entered into the interior of the nanotubes and filled them uniformly. However, no negatively charged particles entered the hollow cylinder at all. This finding strongly suggests that the electrostatic interactions between the nanotubes and particles are crucial for efficient preparation of magnetic nanotubes. Bacterial magnetic Fe_3O_4 nanocrystals were incorporated in the hollow cylinder of the LNT of **2**(*7*).[85] Compared to chemically produced Fe_3O_4 nanocrystals, the bacterial magnetic nanocrystals have a coating layer of proteins on their surface.[86] The protein has a particularly strong affinity toward the applied LNT,[87] facilitating contact of the bacterial magnetic nanocrystals onto

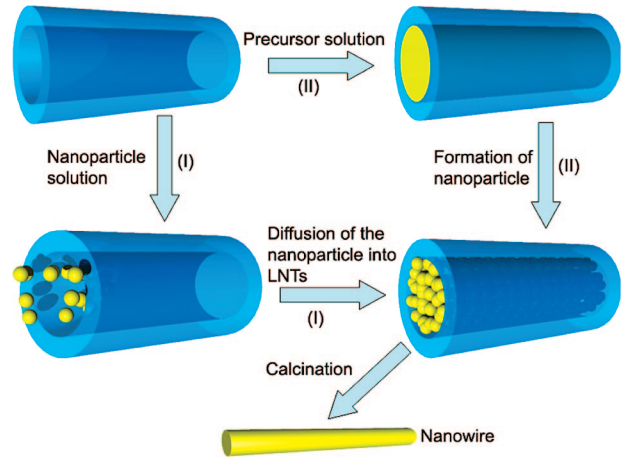

Figure 9. Schematic illustration for the confined 1-D arrangement of NDs and the subsequent formation of the nanowires by using a LNT as a ship-in-bottle scaffold.

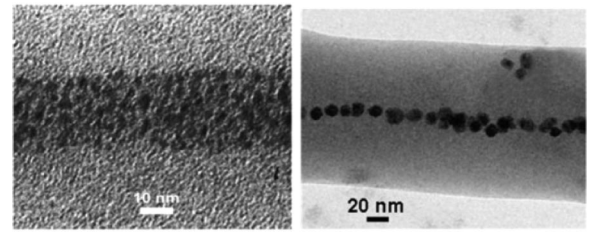

Figure 10. TEM image of the LNT encapsulating the (a) 1−3 nm and (b) 15−20 nm gold NDs into the hollow cylinder, which was produced along path I. Reproduced with permission from ref 82. Copyright 2006 Wiley-VCH.

the LNT surfaces. The bacterial magnetic nanocrystals selectively deposited only to the interior at low concentrations of nanocrystals and to the exterior surfaces of the nanotubes at high concentrations. Such a linear chain of the loaded magnetic nanoparticles introduces a uniaxial magnetic anisotropy, not present in the magnetic particles or assemblies commonly known. We recently designed a functional LNT that possesses both a positively charged inner surface covered with amino groups and a neutral outer surface with hydroxyl groups.[14b,e] The LNT can selectively encapsulate anionic latex beads of sulfate 20 nm in width, DNA, and ferritin proteins in aqueous solutions in the inner hollow cylinder via an electrostatic force. Irrespective of the absence of charged surfaces on the LNT, we have succeeded in filling gold nanoparticles into lyophilized LNTs of **6** that possess both neutral surfaces and a vacant internal channel.[88] To remove the water volume inside the hollow cylinder, we lyophilized the LNT in a vacuum, without damaging the tubular morphologies, and then added the lyophilized LNT into an aqueous solution of gold NDs to make the ND penetrate the nanochannel. This route can allow us to organize the size- and shape-dependent arrays of NDs. Figure 10 shows the remarkable size effect of the gold NDs in the 1-D organization profile in the LNT hollow cylinder. Gold NDs 15–20 nm in width can align side-by-side along the long axis of the LNT hollow 30–50 nm in width, whereas relatively smaller nanoparticles of 1–3 nm width fill the LNT hollow with close packing. Complete removal of the organic LNT shell from the nanocomposite LNT−gold NDs by firing

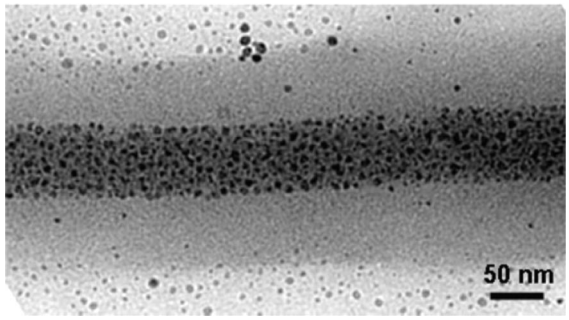

Figure 11. TEM images of the LNT encapsulating the gold NDs into the hollow cylinder, which was produced along path II. Reproduced with permission from ref 82. Copyright 2006 Wiley-VCH.

in air can allow the nanoparticles to remain confined and eventually results in 1-D gold nanowires. The lyophilized LNTs are also capable of loading other metals,[88] semiconductors,[89] ferritin,[90] and magnetic crystals.[91] Path II utilizes the precursor solutions of the payload diffusing into the LNT, followed by in situ formation of NDs in the nanochannels of the LNT. Reches and Gazit performed the self-assembly of the short peptide (NH_2−Phe−Phe−COOH) into stable nanotubes in an organic solution.[57] They loaded silver ions into the hollow section of the peptide nanotube and subsequently reduced the silver ions into silver metal. Proteolysis of the peptide moiety with a proteinase K enzyme results in individual silver nanowires with diameters of 20 nm. They also attached gold nanoparticles on the outer surface of the silver-loaded peptide nanotube with an organic molecular linker.[92] The linker has a diphenylalanine motif, where one end can interact with the peptide nanotube surface by weak noncovalent bonds. The cysteine residue at the other end can provide a reactive thiol group to bind gold nanoparticles covalently. The attached gold nanoparticles then act to initiate site-specific electroless deposition of more gold nanoparticles over the peptide nanotube surfaces. This process leads to the production of trilayered coaxial nanocables [metal (Ag)/insulator (nanotube)/metal (Au)]. Such a coaxial geometry may give rise to useful electromagnetic properties as capacitors. We also loaded gold nanoparticles into the LNTs of **6** along path II.[92] We added the dried LNT powders to 20% aqueous ethanolic solutions containing hydrogen tetrachloroaurate ($HAuCl_4$). This procedure allowed for the filling of the solutions into the vacant LNT hollow by capillary action. Eventually, confined photochemical reduction of Au^{III} to Au^0 in the presence of small amounts of alcohol produced a well-defined LNT filled with gold nanocrystals (Figure 11). Using this strategy, we were also able to produce linear arrays of CdS NDs. By filling a mixture solution of Cd^{2+} and TAA into the LNT and upon resultant formation of CdS, we can organize the CdS NDs along the inner channel of the LNT of **6**.[89]

6. Outlook

Precise self-assembly of amphiphilic monomers can give LNT architectures with well-defined morphologies, controllable dimensions, and designed surface properties. Templating of the LNTs is a promising route to making diverse 1-D nanostructures. The current achievement of the templating method using LNTs has spurred intense and rapid progress in the application. Both utilization of the molecular recognition ability of LNTs and the current development of a 3-D manipulation technique will enable us to connect the templated 1-D nanostructures to external nanodevices in a convenient and precise way in the near future.

Acknowledgment. The authors thank their colleagues Drs. Mitsutoshi Masuda, Hiroyuki Minamikawa, Masumi Asakawa, Masaki Kogiso, Masaru Aoyagi, Bo Yang, Naohiro Kameta, and Qingmin Ji for their continuous support and skillful technique at NARC, AIST, during the course of this work on supramolecular LNTs. Drs. George John, Jong Hwa Jung, Shoko Kamiya, Nikolay V. Goutev, and Hiroharu Yui (CREST-JST) are acknowledged for collaboration on the synthesis and analysis of self-assembled tubular architectures. Drs. Yoshiki Shimizu (AIST) and Kaname Yoshida (Kyoto University) are gratefully acknowledged for carrying out the TEM measurements. Profs. Ichiro Yamashita (Matsushita Electric Industrial) and Kohzo Ito (The University of Tokyo) are also thanked for collaboration on the encapsulation of ferritin into LNTs and on the manipulation of LNTs, respectively. JST is acknowledged for financial support of the CREST and SORST projects.

References

(1) Xia, Y.; Yang, P.; Sun, Y.; Wu, Y.; Mayers, B.; Gates, E.; Yin, Y.; Kim, F.; Yan, H. *Adv. Mater.* **2003**, *15*, 353.
(2) (a) Shimizu, T. *Macromol. Rapid Commun.* **2002**, *23*, 311. (b) Iwaura, R.; Hoeben, F. J. M.; Masuda, M.; Schenning, A. P. H. J.; Meijer, E. W.; Shimizu, T. *J. Am. Chem. Soc.* **2006**, *128*, 13298. (c) Kogiso, M.; Okada, Y.; Yase, K.; Shimizu, T. *J. Colloid Interface Sci.* **2004**, *273*, 394.
(3) Fuhrhop, J. H.; Helfrich, W. *Chem. Rev.* **1993**, *93*, 1565.
(4) Kline, T. R.; Tian, M.; Wang, J.; Sen, A.; Chan, M. W. H.; Mallouk, T. E. *Inorg. Chem.* **2006**, *45*, 7555.
(5) (a) Jung, J. H.; Shinkai, S.; Shimizu, T. *Nano Lett.* **2002**, *2*, 17. (b) John, G.; Masuda, M.; Okada, Y.; Yase, K.; Shimizu, T. *Adv. Mater.* **2001**, *13*, 715.
(6) (a) Martin, C. R. *Chem. Mater.* **1996**, *8*, 1739. (b) Martin, C. R. *Science* **1994**, *266*, 1994.
(7) van Bommel, K. J. C.; Friggeri, A.; Shinkai, S. *Angew. Chem., Int. Ed.* **2003**, *42*, 980.
(8) Yan, H.; Park, S. H.; Finkelstein, G.; Reif, J. H.; LaBean, T. H. *Science* **2003**, *301*, 1882.
(9) Boal, A. K.; Headly, T. J.; Tissot, R. G.; Bunker, B. C. *Adv. Funct. Mater.* **2004**, *14*, 19.
(10) Shenton, W.; Douglas, T.; Young, M.; Stubbs, G.; Mann, S. *Adv. Mater.* **1999**, *11*, 253.
(11) Shimizu, T.; Masuda, M.; Minamikawa, H. *Chem. Rev.* **2005**, *105*, 1401.
(12) Kunitake, T. *Angew. Chem., Int. Ed. Engl.* **1992**, *31*, 709.
(13) (a) Schnur, J. M. *Science* **1993**, *262*, 1669. (b) Spector, M. S.; Price, R. R.; Schnur, J. M. *Adv. Mater.* **1999**, *11*, 337.
(14) (a) Masuda, M.; Shimizu, T. *Langmuir* **2004**, *20*, 5969. (b) Kameta, N.; Masuda, M.; Minamikawa, H.; Goutev, N. V.; Rim, J. A.; Jung, J. H.; Shimizu, T. *Adv. Mater.* **2005**, *17*, 2732. (c) Kameta, N.; Masuda, M.; Minamikawa, H.; Mishima, Y.; Yamashita, I.; Shimizu, T. *Chem. Mater.* **2007**, *19*, 3553. (d) Kameta, N.; Masuda, M.; Minamikawa, H.; Shimizu, T. *Langmuir* **2007**, *23*, 4634. (e) Kameta, N.; Mizuno, G.; Masuda, M.; Minamikawa, H.; Kogiso, M.; Shimizu, T. *Chem. Lett.* **2007**, *36*, 896.
(15) Ijima, S. *Nature* **1991**, *354*, 56.
(16) Wenz, G.; Han, B. H.; Muller, A. *Chem. Rev.* **2006**, *106*, 782.
(17) Ghadiri, M. R.; Granja, J. R.; Milligan, R. A.; McRee, D. E.; Khazanovich, N. *Nature* **1993**, *366*, 324.
(18) Markowitz, M.; Singh, A. *Langmuir* **1991**, *7*, 16.
(19) Singh, A.; Burke, T. G.; Calvert, J. M.; Georger, J. H.; Herendeen, B.; Price, R. R.; Schoen, P. E.; Yager, P. *Chem. Phys. Lipids* **1988**, *47*, 135.
(20) Yang, B.; Kamiya, S.; Yui, H.; Masuda, M.; Shimizu, T. *Chem. Lett.* **2003**, *32*, 1146.
(21) (a) Guo, Y. L.; Yui, H.; Minamikawa, H.; Yang, B.; Masuda, M.; Ito, K.; Shimizu, T. *Chem. Mater.* **2006**, *18*, 1577. (b) Guo, Y.; Yui, H.; Fukagawa, A.; Kamiya, S.; Masuda, M.; Ito, K.; Shimizu, T. *J. Nanosci. Nanotechnol.* **2006**, *6*, 1464.
(22) Porrata, P.; Goun, E.; Matsui, H. *Chem. Mater.* **2002**, *14*, 4378.
(23) Douliez, J. P.; Pontoire, B.; Gaillard, C. *ChemPhysChem.* **2006**, *7*, 2071.
(24) Spector, M. S.; Selinger, J. V.; Singh, A.; Rodriguez, J. M.; Price, R. R.; Schnur, J. M. *Langmuir* **1998**, *14*, 3493.
(25) (a) Frusawa, H.; Fukagawa, A.; Ikeda, Y.; Araki, J.; Ito, K.; John, G.; Shimizu, T. *Angew. Chem., Int. Ed.* **2003**, *42*, 72. (b) Fujima, T.; Frusawa, H.; Minamikawa, H.; Ito, K.; Shimizu, T. *J. Phys.: Condens. Matter* **2006**, *18*, 3089.

(26) (a) Mahajan, N.; Fang, J. *Y. Langmuir* **2005**, *21*, 3153. (b) Zhao, Y.; Fang, J. Y. *Langmuir* **2006**, *22*, 1891. (c) Fang, J. Y. *J. Mater. Chem.* **2007**, *17*, 3479.
(27) Brazhnik, K. P.; Vreeland, W. N.; Hutchison, J. B.; Kishore, R.; Wells, J.; Helmerson, K.; Locascio, L. E. *Langmuir* **2005**, *21*, 10841.
(28) Reches, M.; Gazit, E. *Nat. Nanotech.* **2006**, *1*, 195.
(29) Rosenblatt, C.; Yager, P.; Schoen, P. E. *Biophys. J.* **1987**, *52*, 295.
(30) Matsui, H.; Porrata, P.; Douberly, G. E. J. *Nano Lett.* **2001**, *1*, 461.
(31) Schnur, J. M.; Price, R.; Schoen, P.; Yager, P.; Calvert, J. M.; Georger, J.; Singh, A. *Thin Solid Films* **1987**, *152*, 181.
(32) Matsui, H.; Pan, S.; Gologan, B.; Jonas, S. *J. Phys. Chem. B* **2000**, *104*, 9576.
(33) Zabetakis, D. *J. Mater. Res.* **2000**, *15*, 2368.
(34) Chow, G. M.; Stockton, W. B.; Price, R.; Baral, S.; Ting, A. C.; Ratna, B. R.; Shoen, P. E.; Schnur, J. M.; Bergeron, G. L.; Czarnaski, M. A.; Hickman, J. J.; Kirkpatrick, D. A. *Mater. Sci. Eng. A* **1992**, *158*, 1.
(35) (a) Price, R. R.; Patchan, M. *J. Microencapsulation* **1991**, *8*, 301. (b) Ahl, P. L.; Price, R. R.; Smuda, J.; Gaber, B. P.; Singh, A. *Biochim. Biophys. Acta* **1990**, *1028*, 141.
(36) Matsui, H.; Pan, S.; Douberly, G. E., Jr. *J. Phys. Chem. B* **2001**, *105*, 1683.
(37) (a) Shimizu, T.; Kogiso, M.; Masuda, M. *Nature* **1996**, *383*, 487. (b) Kogiso, M.; Ohnishi, S.; Yase, K.; Masuda, M.; Shimizu, T. *Langmuir* **1998**, *14*, 4978.
(38) Gao, X.; Matsui, H. *Adv. Mater.* **2005**, *17*, 2037.
(39) (a) Banerjee, I. A.; Yu, L.; Matsui, H. *Proc. Natl. Acad. Sci. U.S.A.* **2002**, *99*, 6451. (b) Yu, L.; Banerjee, I. A.; Shima, M.; Rajan, K.; Matsui, H. *Adv. Mater.* **2004**, *16*, 709.
(40) Yu, L.; Banerjee, I. A.; Matsui, H. *J. Am. Chem. Soc.* **2003**, *125*, 14837.
(41) (a) Djalali, R.; Chen, Y.; Matsui, H. *J. Am. Chem. Soc.* **2002**, *124*, 13660. (b) Dajali, R.; Chen, Y.; Matsui, H. *J. Am. Chem. Soc.* **2003**, *125*, 5873.
(42) Banerjee, I. A.; Yu, L.; Matsui, H. *J. Am. Chem. Soc.* **2005**, *127*, 16002.
(43) Gao, X.; Djalali, R.; Haboosheh, A.; Samson, J.; Nuraje, N.; Matsui, H. *Adv. Mater.* **2005**, *17*, 1753.
(44) Chappell, J. S.; Yager, P. *J. Mater. Sci.* **1992**, *11*, 633.
(45) (a) Baral, S.; Schoen, P. *Chem. Mater.* **1993**, *5*, 145. (b) Zhao, Y.; Liu, J.; Sohn, Y.; Fang, J. *J. Phys. Chem. C* **2007**, *111*, 6418.
(46) Archibald, D. D.; Mann, S. *Nature* **1993**, *364*, 430.
(47) Patil, A. J.; Muthusamy, E.; Seddon, A. M.; Mann, S. *Adv. Mater.* **2003**, *15*, 1816.
(48) Ji, Q.; Iwaura, R.; Kogiso, M.; Jung, J. H.; Yoshida, K.; Shimizu, T. *Chem. Mater.* **2004**, *16*, 250.
(49) Ji, Q.; Iwaura, R.; Shimizu, T. *Chem. Lett.* **2004**, 504.
(50) Ji, Q.; Iwaura, R.; Shimizu, T. *Chem. Mater.* **2007**, *19*, 1329.
(51) Ji, Q.; Shimizu, T. *Chem. Commun.* **2005**, 4411.
(52) (a) Kamiya, S.; Minamikawa, H.; Jung, J. H.; Yang, B.; Masuda, M.; Shimizu, T. *Langmuir* **2005**, *21*, 743. (b) Ji, Q.; Kamiya, S.; Shimizu, T. *Chem. Lett.* **2006**, *35*, 394.
(53) Ji, Q. M.; Kamiya, S.; Jung, J. H.; Shimizu, T. *J. Mater. Chem.* **2005**, *15*, 743.
(54) Zhou, Y.; Kogiso, M.; He, C.; Shimizu, Y.; Koshizaki, N.; Shimizu, T. *Adv. Mater.* **2007**, *19*, 1055.
(55) Kogiso, M.; Zhou, Y.; Shimizu, T. *Adv. Mater.* **2007**, *19*, 242.
(56) Song, Y.; Challa, S. R.; Medforth, C. J.; Qiu, Y.; Watt, R. K.; Peña Miller, J. E.; van Swol, F.; Shelnutt, J. A. *Chem. Commun.* **2004**, 1044.
(57) (a) Reches, M.; Gazit, E. *Science* **2003**, *300*, 625. (b) Yan, X.; He, Q.; Wang, K.; Duan, L.; Cui, Y.; Li, J. *Angew. Chem., Int. Ed.* **2007**, *46*, 2431.
(58) Seddon, A. M.; Patel, H. M.; Burkett, S. L.; Mann, S. *Angew. Chem., Int. Ed.* **2002**, *41*, 2988.
(59) Lin, T. F.; Ho, R. M.; Sung, C. H.; Hsu, C. S. *Chem. Mater.* **2006**, *18*, 5510.
(60) Aikawa, K.; Mikami, K. *Angew. Chem., Int. Ed.* **2003**, *42*, 5458.
(61) Yu, S. H.; Colfen, H.; Tauer, K.; Antonietti, M. *Nat. Mater.* **2005**, *4*, 51.
(62) Cornell, B. A.; Braach-Maksvytis, V. L. B.; King, L. G.; Osman, P. D. J.; Raguse, B.; Wieczorek, L.; Pace, J. *Nature* **1997**, *87*, 580.
(63) Gao, P. M.; Ding, Y.; Mai, W. J.; Hughes, W. L.; Lao, C. S.; Wang, Z. L. *Science* **2005**, *309*, 1700.
(64) Hodgekinson, I.; Wu, Q. H. *Adv. Mater.* **2001**, *13*, 889.
(65) (a) Kawano, S. I.; Tamaru, S. I.; Fujita, N.; Shinkai, S. *Chem.—Eur. J.* **2004**, *10*, 343. (b) Jung, J. H.; Lee, S. H.; Yoo, J. S.; Yoshida, K.; Shimizu, T.; Shinkai, S. *Chem.—Eur. J.* **2003**, *9*, 5307. (c) Jung, J. H.; Shinkai, S.; Shimizu, T. *Chem. Mater.* **2003**, *15*, 2141. (d) Jung, J. H.; Shinkai, S.; Shimizu, T. *Chem. Rec.* **2003**, *3*, 212. (e) Jung, J. H.; Ono, Y.; Hanabusa, K.; Shinkai, S. *J. Am. Chem. Soc.* **2000**, *122*, 5008. (f) Jung, J. H.; Ono, Y.; Shinkai, S. *Chem.—Eur. J.* **2000**, *6*, 4552. (g) Jung, J. H.; Shimizu, T.; Shinkai, S. *J. Mater. Chem.* **2005**, *15*, 3979.
(66) Kobayashi, S.; Hamasaki, N.; Suzuki, M.; Kimura, M.; Shirai, H.; Hanabusa, K. *J. Am. Chem. Soc.* **2002**, *124*, 6550.
(67) Sone, E. D.; Zubarev, E. R.; Stupp, S. I. *Angew. Chem., Int. Ed.* **2002**, *41*, 1706.
(68) Fu, X.; Wang, Y.; Huang, L.; Sha, Y.; Gui, L.; Lao, L.; Tang, Y. *Adv. Mater.* **2003**, *15*, 902.
(69) Selinger, J. V.; Schnur, J. M. *Phys. Rev. Lett.* **1993**, *71*, 4091.
(70) Burkett, S. L.; Mann, S. *Chem. Commun.* **1996**, 321.
(71) Lvov, Y. M.; Price, R. R.; Selinger, J. V.; Singh, A.; Spector, M. S.; Schnur, J. M. *Langmuir* **2000**, *16*, 5932.
(72) (a) Zhu, H. F.; Ai, S. F.; He, Q.; Cui, Y.; Li, J. B. *J. Nanosci. Nanotechnol.* **2007**, *7*, 2361. (b) Ai, S. F.; He, Q.; Tian, Y.; Li, J. B. *J. Nanosci. Nanotechnol.* **2007**, *7*, 2534. (c) Cui, Y.; Tao, C.; Tian, Y.; He, Q.; Li, J. B. *Langmuir* **2006**, *22*, 8205. (d) Tian, Y.; He, Q.; Tao, C.; Li, J. B. *Langmuir* **2006**, *22*, 360. (e) Li, J. B.; Cui, Y. *J. Nanosci. Nanotechnol.* **2006**, *6*, 1552. (f) Tian, Y.; He, Q.; Cui, Y.; Tao, C.; Li, J. B. *Chem.—Eur. J.* **2006**, *12*, 4808. (g) Lu, G.; Ai, S. F.; Li, J. B. *Langmuir* **2005**, *21*, 1679. (h) Ai, S. F.; He, Q.; Tao, C.; Zheng, S. P.; Li, J. B. *Macromol. Rapid Commun.* **2005**, *26*, 1965. (i) Ai, S. F.; Lu, G.; He, Q.; Li, J. B. *J. Am. Chem. Soc.* **2003**, *125*, 11140.
(73) Price, R. R.; Dressick, W. J.; Singh, A. *J. Am. Chem. Soc.* **2003**, *125*, 11259.
(74) Jung, J. H.; Rim, J. A.; Lee, S. J.; Lee, S. S. *Chem. Commun.* **2005**, 468.
(75) Zhou, Y.; Ji, Q.; Masuda, M.; Kamiya, S.; Shimizu, T. *Chem. Mater.* **2006**, *18*, 403.
(76) Goren, M.; Qi, Z.; Lennox, R. B. *Chem. Mater.* **2000**, *12*, 1222.
(77) (a) Sada, K.; Takeuchi, M.; Fujita, N.; Numata, M.; Shinkai, S. *Chem. Soc. Rev.* **2007**, *36*, 415. (b) Hatano, T.; Bae, A. H.; Takeuchi, M.; Fujita, N.; Kaneko, K.; Ihara, H.; Takafuji, M.; Shinkai, S. *Angew. Chem., Int. Ed.* **2004**, *43*, 465. (c) Hatano, T.; Bae, A. H.; Takeuchi, M.; Fujita, N.; Kaneko, K.; Ihara, H.; Takafuji, M.; Shinkai, S. *Chem.—Eur. J.* **2004**, *10*, 5067.
(78) Ringler, P.; Müller, W.; Ringsdorf, H.; Brisson, A. *Chem.—Eur. J.* **1997**, *3*, 620.
(79) DeRosier, D. J.; Moore, P. B. *J. Mol. Biol.* **1970**, *52*, 355.
(80) Wilson-Kubalek, E. M.; Brown, R. E.; Celia, H.; Milligan, R. A. *Proc. Natl. Acad. Sci. U.S.A.* **1998**, *95*, 8040.
(81) Shchukin, D. G.; Sukhorukov, G. B. *Adv. Mater.* **2004**, *16*, 671.
(82) Shimizu, T. *J. Polym. Sci., Part A* **2006**, *44*, 5137.
(83) Zarif, L. *J. Controlled Release* **2002**, *81*, 7.
(84) Letelliner, D.; Sandre, O.; Menager, C.; Cabuil, V.; Lavergne, M. *Mater. Sci. Eng.* **1997**, *5*, 153.
(85) Banerjee, I. A.; Yu, L.; Shima, M.; Yoshino, T.; Takeyama, H.; Matsunaga, T.; Matsui, H. *Adv. Mater.* **2005**, *17*, 1128.
(86) Yang, C. D.; Takeyama, H.; Tanaka, T.; Matsunaga, T. *Enzyme Microb. Technol.* **2001**, *29*, 13.
(87) Douberly, G. E.; Pan, S.; Walters, D.; Matsui, H. *J. Phys. Chem. B* **2001**, *105*, 7612.
(88) Yang, B.; Kamiya, S.; Shimizu, Y.; Koshizaki, N.; Shimizu, T. *Chem. Mater.* **2004**, 2826.
(89) Zhou, Y.; Kamiya, S.; Shimizu, T. Unpublished results.
(90) Yui, H.; Shimizu, Y.; Kamiya, S.; Masuda, M.; Yamshita, I.; Ito, K.; Shimizu, T. *Chem. Lett.* **2005**, *34*, 232.
(91) Yui, H.; Shimizu, Y. Unpublished results.
(92) Carny, O.; Shalev, D. E.; Gazit, E. *Nano Lett.* **2006**, *6*, 1594.
(93) Yang, B.; Kamiya, S.; Yoshida, K.; Shimizu, T. *Chem. Commun.* **2004**, 500.

CM701999M